Journal of Physical Science, Vol. 27(3), 97–119, 2016

Investigation of Gamma Radiation Shielding Properties of Some Zinc Tellurite Glasses

Shams Issa,[1,2*] Mohamad Sayyed[2] and Murat Kurudirek[3]

[1] Physics Department, Faculty of Science, Al-Azhar University, 71524 Assiut, Egypt
[2]Physics Department, Faculty of Science, University of Tabuk, 71491 Tabuk, Saudi Arabia
[3]Faculty of Science, Department of Physics, Ataturk University, 25240 Erzurum, Turkey

[*]Corresponding author: shams_issa@yahoo.com

Published online: 25 November 2016

To cite this article: Issa, S. et al. (2016). Investigation of gamma radiation shielding properties of some zinc tellurite glasses. *J. Phys. Sci.*, 27(3), 97–119, http://dx.doi.org/10.21315/jps2016.27.3.7

To link to this article: http://dx.doi.org/10.21315/jps2016.27.3.7

ABSTRACT: *The mass attenuation coefficient (μ_m), half-value layer (HVL) and mean free path for xZnO-(100-x) TeO_2, where x = 10, 20, 30, and 40 mol.%, have been measured with 0.662, 1.173 and 1.33 MeV photons emitted from ^{137}Cs and ^{60}Co using a 3 × 3 inch NaI(Tl) detector. Some relevant parameters, such as the effective atomic numbers (Z_{eff}) and electron densities (N_{el}), of the glass samples have also been calculated in the photon energy range of 0.015–15 MeV. Moreover, exposure buildup factors (EBF) were estimated using the five-parameter Geometric Progression (G-P) fitting approximation for penetration depths up to 40 times the mean free path and within the same energy range of 0.015–15 MeV. The measured mass attenuation coefficients were found to agree satisfactorily with the theoretical values obtained using WinXCom. The effective atomic numbers (Z_{eff}) and electron densities (N_{el}) were found to be the highest for a 40ZnO-60TeO_2 glass in the energy range of 0.04–0.2 MeV. The 10ZnO-90TeO_2 glass sample had lower values of gamma ray exposure buildup factors in the intermediate energy region. These data on the radiation shielding characteristics of zinc tellurite glasses may be useful for the design of gamma radiation shields.*

Keywords: Mass attenuation coefficient, effective atomic number, electron density, exposure buildup factors, tellurite glass

1. INTRODUCTION

High-energy gamma rays are a type of electromagnetic radiation, emitted by radioisotopes or other radiation sources, that can travel distances of many kilometres within seconds. Gamma ray emitting isotopes have been used extensively in many fields, such as industry, agriculture and medicine. It is very important to develop effective mixtures of materials that can act as shields against such nuclear radiation.[1–3] Materials having high atomic-number constituents, such as tellurite (Z = 52), are widely used in radiation shields due to their strong attenuation of X-rays, gamma rays and fast neutrons.[4] The preparation and modification of transparent glasses are essential for the development of a proper radiation shield. Tellurites transmit wavelengths in the range of 0.5 μm to 6 μm, display good mechanical and thermal stability and are not photosensitive.[5–9] The addition of ZnO to tellurite increases glass formation and thermal stability.[10,11]

The gamma radiation shielding properties of different compounds were evaluated using parameters, such as mass attenuation coefficient (μ_m), half-value layer (HVL), effective atomic number (Z_{eff}), electron density (N_{el}) and buildup factors (BFs).[12] The EBF refers to the exposure in the air after penetration through the absorber or shielding material. Since a primary assessment of radiation protection is the exposure field before and after the use of a radiation shield, exposure buildup factors are often of more general use, with appropriate adjustments for air exposure, to obtain the absorbed dose.[13] The build-up factor values have been computed by various codes, such as the Geometric Progression (GP) method,[14] iterative method,[15] invariant embedding method,[16,17] and Monte Carlo method.[18] The American National Standards ANSI/ANS 6.4.3[19] used a GP fitting method and provided build-up factor data for 23 elements, along with water, air and concrete, at 25 standard energies in the energy range of 0.015–15 MeV, with suitable intervals, up to a penetration depth of 40 mean free paths.

While several studies have been performed to investigate the degree of radiation attenuation in different glass samples,[20–25] the radiation shielding characteristics of the selected zinc tellurite glasses have not yet been investigated yet, which prompted us to carry out this work. In the present work, the mass attenuation coefficients were measured for tellurite glasses at photon energies of 0.662, 1.173 and 1.33 MeV. The effective atomic numbers (Z_{eff}) and electron densities (N_{el}) of the glass samples were calculated in the energy range of 0.015–15 MeV. The gamma ray exposure buildup factors (EBF) of the glass systems were computed for penetration depths up to 40 mean free paths in the energy range of 0.015–15 MeV.

2. EXPERIMENTAL

2.1 Sample Preparation

The glass systems made of composite xZnO-(100-x)TeO_2, where x = 10, 20, 30, and 40 mol%, were prepared by a rapid melt quenching technique using TeO_2 and ZnO (99.99%). Exact mole ratios of the reactants were mixed thoroughly with an agate mortar. The mixtures were initially heated in a ceramic crucible in an electrical muffle furnace at 1073K for 60 min, and the melt was swirled frequently to ensure proper mixing and homogeneity. The melt was then quenched to room temperature. The obtained samples were annealed by transferring them into another electrical furnace at a temperature of 623K for 4 h and slowly cooling to room temperature to minimise the cracking and thermal stress of the glasses.[26–28] The samples were prepared with different thicknesses (0.5–1.3 cm). The relative error in the thickness was found to be ±0.002 cm. The densities of the prepared glassy samples were determined by the Archimedes method via immersion in a liquid, such as acetone. The chemical composition of the glass samples, densities, molar volume and thickness are listed in Table 1.

Table 1: Chemical composition, density, molar volume (M_v) and thickness of glass samples.

Sample	Composition (mole fraction)		Density ρ (g cm^{-3})	M_v (cm^3 mol^{-1})	Thickness* (cm)
	ZnO	TeO_2			
1	10	90	5.048 ± 0.050	30.067	0.523
2	20	80	5.101 ± 0.051	28.221	0.752
3	30	70	5.149 ± 0.051	26.439	0.912
4	40	60	5.181 ± 0.052	24.766	1.321

**The relative error in the thickness error was found as ±0.002 cm*

2.2 Measurements

The mass attenuation coefficient measurements were performed with a gamma ray spectrometer, which employed a scintillation detector (3 × 3 inch) (Figure 1). The hermetically sealed assembly included a high-resolution NaI (Tl) crystal, photomultiplier tube, internal magnetic/light shield, aluminium housing and a 14-pin connector coupled to PC-MCA Canberra Accuspec. It had the following specifications: (1) resolution 7.5%, specified at the 662 keV peak of ^{137}Cs; (2) an aluminium window 0.5 mm thick, with a density of 147 mg cm^{-2}; (3) a 1.6 mm thick reflector oxide with a density of 88 mg cm^{-2}; (4) a conical lined steel magnetic/light shield; and (5) a +902 volt DC operating voltage. A dedicated software program, Genie 2000 from Canberra, was used to carry out the on-line

analysis of each measured gamma ray spectrum. The detection array was energy calibrated using ^{60}Co (1173.2 and 1332.5 keV), ^{133}Ba (356.1 keV) and ^{137}Cs (661.9 keV).

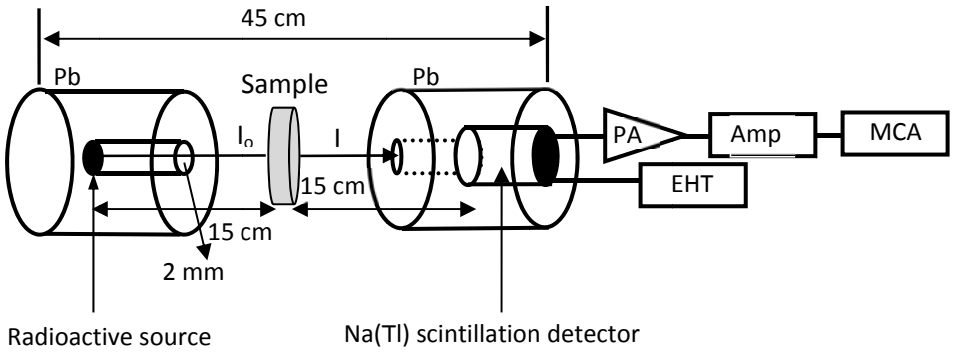

Figure 1: Narrow beam experiment geometry.

The experimental mass attenuation coefficients (μ_m) of the glass samples have been measured by the well-known Beer-Lambert equation:

$$\mu_m = \frac{\ln(I_o/I)}{\rho t} \tag{1}$$

Where I_0 and I are the incident and transmitted intensities, ρ is the density of material (g cm^{-3}) and t is the thickness of the absorber (cm). The glass samples were irradiated by 0.662, 1.173 and 1.33 MeV photons from 5 μCi ^{137}Cs and ^{60}Co radioactive sources. The measurements were taken for four hours and were repeated 5 times for each sample.

3. CALCULATIONS

3.1 Effective Atomic Number and Electron Density

The total photon interaction cross section (σ_t) of the glasses was determined using the mass attenuation coefficient (μ_m) via the following equation:

$$\sigma_t = \frac{M\mu_m}{N_A} \tag{2}$$

Where $M = \sum_i A_i n_i$ is the molecular weight of the sample, A_i is the atomic weight of the i-th element, n_i is the number of formula units of the molecule and N_A is Avogadro's number.

The effective atomic cross section σ_a is calculated using the following equation:

$$\sigma_a = \frac{\sigma_t}{\sum_i n_i} \tag{3}$$

The total electronic cross section σ_e is calculated by:

$$\sigma_e = \frac{1}{N_A} \sum_i \frac{f_i A_i}{Z_i} (\mu_m)_i \tag{4}$$

where f_i denotes the fractional abundance of element I, and Z_i is the atomic number of the constituent element.

The effective atomic number (Z_{eff}) is related to σ_a and σ_e by the following equation:

$$Z_{eff} = \frac{\sigma_a}{\sigma_e} \tag{5}$$

The electron density (number of electrons per unit mass, [N_{el}]) of the sample can be calculated by the following equation:

$$N_{el} = \frac{Z_{eff} N_A}{M} \sum_i n_i \left(\frac{electrons}{g} \right) \tag{6}$$

3.2. Buildup Factors

The logarithmic interpolation method for the equivalent atomic number (Z_{eq}) was used to calculate the exposure buildup factor values and the G-P fitting parameters of the tellurite glass samples. The computation method is illustrated step-by-step as follows:

1. Calculation of equivalent atomic number (Z_{eq});
2. Calculation of the G-P fitting parameters; and
3. Calculation of the exposure buildup factors

Since any single element has a fixed atomic number Z, a mixture, such as the zinc tellurite glasses studied here, will have an equivalent atomic number (Z_{eq}), which describes the properties the of glass systems. Because the partial interaction of a gamma ray with a material depends on the energy, Z_{eq} is an energy dependent parameter. Using the winXCom program,[29,30] the total mass attenuation coefficient of selected $ZnO\text{-}TeO_2$ glasses and Compton partial mass attenuation coefficient for elements from Z = 4 to Z = 50 were obtained in the energy range of 0.015–15 MeV. The equivalent atomic number was calculated by matching the ratio of the Compton partial mass attenuation coefficient to the total mass attenuation coefficient of the selected glass systems with an identical ratio of a single element of the same energy. The following formula was used to interpolate the Zeq:[31]

$$Z_{eq} = \frac{Z_1\left(\log R_2 - \log R\right) + Z_2\left(\log R - \log R_1\right)}{\log R_2 - \log R_1} \tag{7}$$

where Z_1 and Z_2 are the atomic numbers of the elements corresponding to the ratios R_1 and R_2, respectively, and R is the ratio of the glass sample at a specific energy. For example, the ratio $(\mu/\rho)_{Compton}/(\mu/\rho)_{total}$ of $10ZnO\text{-}90TeO_2$ at an energy of 0.3 MeV is 0.635, which lies between $R_1 = (\mu/\rho)_{Compton}/(\mu/\rho)_{total} = 0.628$ of $Z_1 = 46$ and $R_2 = (\mu/\rho)_{Compton}/(\mu/\rho)_{total} = 0.645$ of Z = 47. Using Equation 7, $Z_{eq} = 46.42$ is calculated. The G-P fitting parameters are calculated using a similar logarithmic interpolation method to that used for Z_{eq}. The G-P fitting parameters for the elements were taken from a report by the American Nuclear Society.[19] The G-P fitting parameters for the glass samples were logarithmically interpolated using the same formula as follows:[31]

$$C = \frac{C_1\left(\log Z_2 - \log Z_{eq}\right) + C_2\left(\log Z_{eq} - \log Z_1\right)}{\log Z_2 - \log Z_1} \tag{8}$$

where C_1 and C_2 are the values of the G-P fitting parameters corresponding to the atomic numbers of Z_1 and Z_2, respectively, at a given energy. The G-P fitting parameters were used to calculate the exposure buildup factors of the glasses as follows:[32]

$$B(E,X) = 1 + \frac{b-1}{K-1}\left(K^x - 1\right) \qquad \text{for } K \neq 1 \tag{9}$$

$$B(K,X) = 1 + (b-1)x \qquad \text{for } K = 1 \tag{10}$$

where,

$$K(E,x) = cx^{\alpha} + d\frac{\tan h\left(\frac{x}{X_K} - 2\right) - \tan h(-2)}{1 - \tan h(-2)} \qquad \text{for } x \le 40mfp \qquad (11)$$

where E is the incident photon energy and x is the penetration depth in mfp. Variables a through d, along with X_k, are the G-P fitting parameters. The variation of the parameter K with the penetration depth represents the photon dose multiplication and a change in the shape of the spectrum.

4. RESULTS AND DISCUSSION

The density (ρ) and the molar volume (M_v) of the investigated glasses are listed in Table 1. It is observed that the density of the glass increased from 5.048–5.181 (g m^{-3}) with the substitution of TeO_2 by ZnO, while the molar volume decreased from 30.067 to 24.766 (cm^3 mol^{-1}). The increase in density indicates that the zinc ions entered the tellurite glass network, which is related to the variation of the molar volume of the samples. The decrease in the molar volume is due to the decrease in the bond length, or inter-atomic spacing, between the atoms, which may be attributed to an increase in the stretching force constant (216–217.5 N m^{-1}) of the bonds inside the glass network. Hence, the radius of the Zn^{2+} (0.074 nm) ions is much smaller than that of Te^{2+} (0.097 nm), resulting in a more compact and dense glass. The addition of ZnO is probably caused by a change in the crosslink density and coordination number of the Te^{2+} ions.[31]

4.1 Mass Attenuation Coefficient (μ_M)

The experimental and theoretical values of the mass attenuation coefficients for the four glass samples at gamma energies of 0.662, 1.173 and 1.33 MeV are given in Table 2. The theoretical values of the mass attenuation coefficients were calculated using WinXCom.[28] The estimated error in the experimental measurements was ≤ 2%. It is clear from Table 2 that the mass attenuation coefficients of the glass samples decreased with increasing gamma energy. At a low photon energy, the most important reaction between the studied glass samples and the gamma rays was the photoelectric effect, which decreases with increasing gamma energy. The behaviour of the mass attenuation coefficient at intermediate photon energies may be attributed to a Compton scattering process. The values of the mass attenuation coefficient are dependent on the elemental

composition and, consequently, on the glass density.[32] The experimental values (μ_m) increased with increasing ZnO content. This behaviour may be attributed to the addition of ZnO, which increases the glass density and decreases the molar volume, indicating that the glass structure becomes more compact and dense. The experimental mass attenuation coefficient values are in good agreement with the theoretical values.

Table 2: Theoretical $(\mu_m)_{Xcom}$ and experimental $(\mu_m)_{exp}$ mass attenuation coefficient of glass systems.

Sample	0.662 MeV		1.173 MeV		1.33 MeV	
	$\mu_m \times 10^{-2}$ ($cm^2\ g^{-1}$)					
	WinXcom	Exp.	WinXcom	Exp.	WinXcom	Exp.
1	7.272	7.138 ± 0.134	5.322	5.216 ± 0.106	4.971	4.872 ± 0.099
2	7.275	7.149 ± 0.126	5.347	5.239 ± 0.108	4.998	4.898 ± 0.100
3	7.279	7.142 ± 0.137	5.386	5.277 ± 0.109	5.037	4.936 ± 0.101
4	7.28	7.139 ± 0.141	5.399	5.305 ± 0.094	5.050	4.949 ± 0.101

4.2 HVL and MFP

The half-value layer was calculated using the linear attenuation coefficient (in cm^{-1}) as follows:

$$HVL = \frac{\ln(2)}{\mu} \tag{12}$$

Where μ ($\mu = \rho \times \mu_m$) is the linear attenuation coefficient, and the values of HVL are listed in Table 3. Figure 2 shows that the HVL values decreased with increasing values of ZnO in the glass systems at the photon energies of 0.662, 1.173 and 1.33 MeV, which is due to an increase in the mass attenuation coefficient and density by replacing TeO_2 with ZnO. As shown in Figure 2, the half-value layer of the glass samples is lower than the corresponding values for barite and ferrite concretes at 0.662 and 1.33 MeV photon energies.[22] It has been observed that ZnO-TeO_2 class systems are better than concrete at absorbing gamma rays, indicating the potential for utilising the prepared glasses as radiation shields.

Table 3: HVL and MFP of glass systems.

Sample	HVL (cm)			MFP (cm)		
	0.662 MeV	1.173 MeV	1.330 MeV	0.662 MeV	1.173 MeV	1.330 MeV
1	1.893	2.590	2.773	2.73	3.74	4.00
2	1.870	2.546	2.724	2.70	3.67	3.93
3	1.852	2.509	2.684	2.67	3.62	3.87
4	1.839	2.480	2.651	2.65	3.58	3.83

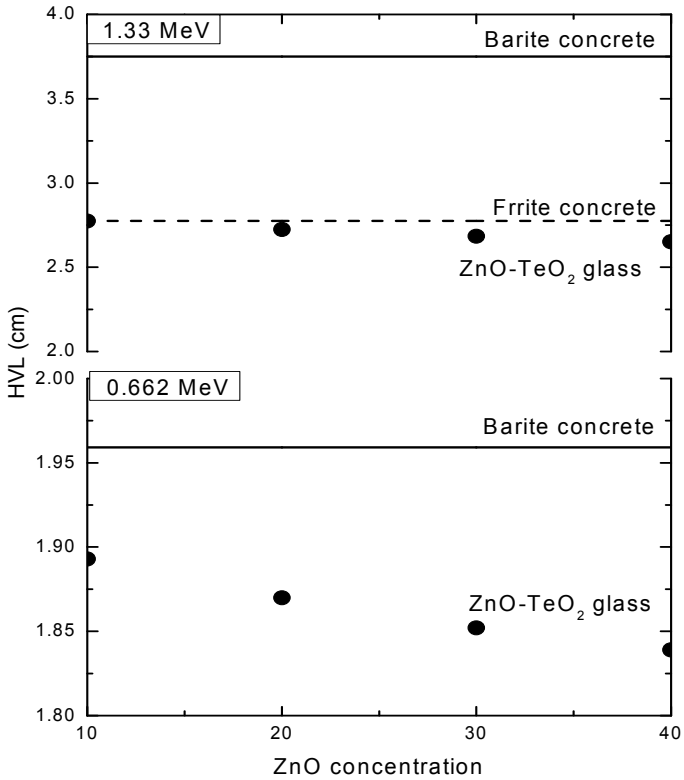

Figure 2: Variation of half value layer as a function of ZnO at 0.662 and 1.33 MeV photon energy in the (•) $ZnO\text{-}TeO_2$ glass systems. Theoretical values at same energies for barite concrete and ferrite concrete.

The values of the mean free path (MFP) (cm^{-1}) of the prepared glass samples were obtained using the following equation:[31]

$$MFP = \frac{1}{\mu} \tag{13}$$

Table 3 shows that the values of the mean free path of the prepared glass samples decreased with increasing ZnO content. The MFP values of the ZnO-TeO_2 glasses were compared with some standard radiation shielding concretes[33] (Figure 3). Figure 3 shows that the values of the mean free path are lower than those in ilmenite, basalt-magnetite, haematite-serpentine and ordinary concretes at 0.662, 1.173, and 1.33 MeV photon energies. This result indicates that the glass samples are better radiation shielding materials compared with standard shielding concretes. A material to be used as a gamma ray radiation shielding material must have low values of HVL and MFP. Therefore, the results indicated that ZnO-TeO_2 glass systems, which show lower values of HVL and MFP at photon energy 0.662, 1.173 and 1.33 MeV, are better for gamma ray shielding. Hence, it is thought that the prepared glass samples can be promising candidates for non-conventional alternatives for gamma ray shielding applications.

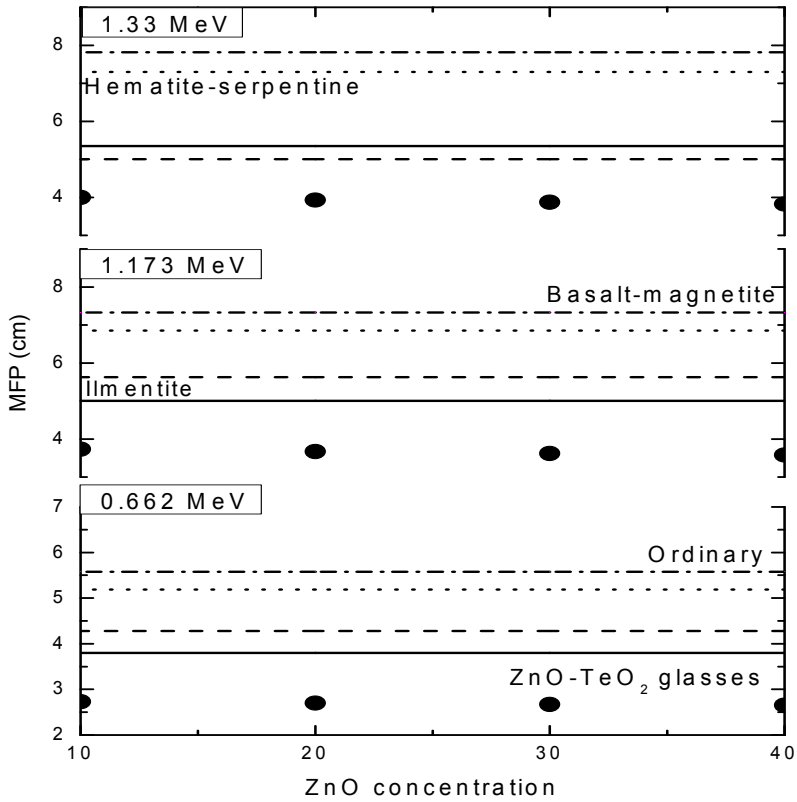

Figure 3: Variation of mean free path as a function of ZnO oxide at 0.662, 1.173 and 1.33 MeV photon energy in the (•) ZnO-TeO_2 glass systems. Theoretical values at same energies for ordinary concrete, hematite-serpentine, basalt-magnetite and ilmentite.

4.3 Effective Atomic Number (Z_{eff}) and Electron Density (N_{el})

The effective atomic number (Z_{eff}) and electron density (N_{el}) of the glass samples in the energy range of 0.015–15 MeV are presented in Table 4. Equations 5 and 6 have been used, respectively, to calculate the effective atomic number (Z_{eff}) and electron density (N_{el}). The variation of Z_{eff} with photon energy for all interaction processes in the glasses is shown in Figure 4. It can be observed that initially, the photoelectric interaction dominates and the effective atomic number remains almost constant in the energy range of 0.015–0.03 MeV. Then, it starts increasing and reaches a maximum at 0.04 MeV. Finally, it decreases sharply with increasing energy up to 1 MeV, which indicates that the Compton scattering process begins to occur. In the intermediate energy region (0.6–2 MeV), the Z_{eff} values have been found to be almost constant for the selected materials, which clearly indicates that the Compton scattering cross section depends only on the energy and is almost independent of the composition of the materials. Finally, the effective atomic number increased with increasing photon energy. This is due to the domination of the pair production process, whose cross section is proportional with Z^2. Figure 4 shows that in the photon energy range 0.04–0.6 MeV, the 10ZnO-90TeO_2 glass sample has the highest effective atomic number. The variation of electron density when investigating glass systems with photons in the range of 0.015–15 MeV have demonstrated the same behaviour of Z_{eff} as shown in Figure 5.

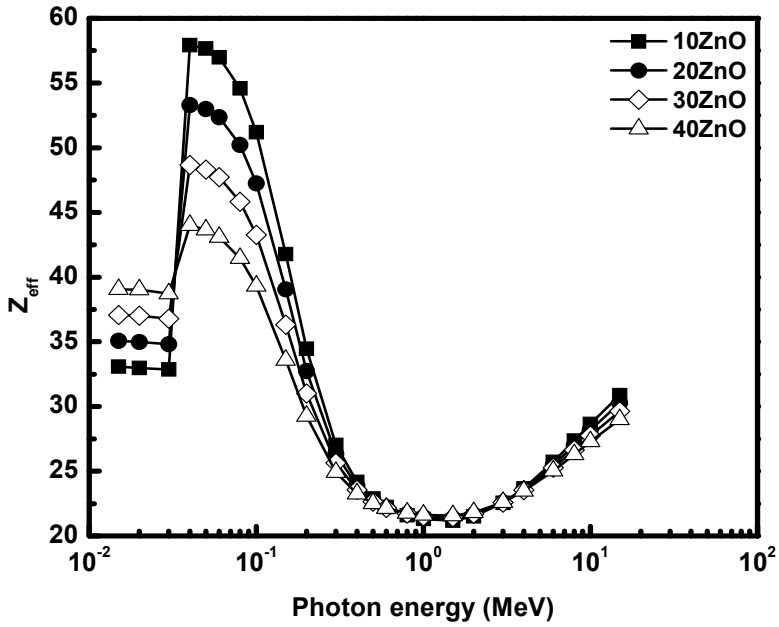

Figure 4: The variation of Z_{eff} with photon energy of glass samples.

Table 4: Effective atomic number (Z_{eff}) and electron density (N_{el}) × 10^{23} of glass samples.

Energy (MeV)	10ZnO		20ZnO		30ZnO		40ZnO	
	Z_{eff}	N_{el}	Z_{eff}	N_{el}	Z_{eff}	N_{el}	Z_{eff}	N_{el}
0.015	33.087	4.134	35.074	4.382	37.062	4.631	39.050	4.879
0.02	32.977	4.120	34.995	4.372	37.012	4.624	39.029	4.876
0.03	32.859	4.106	34.816	4.350	36.773	4.595	38.730	4.839
0.04	57.927	7.238	53.289	6.658	48.652	6.079	44.014	5.499
0.05	57.667	7.205	52.995	6.621	48.322	6.038	43.650	5.454
0.06	56.989	7.120	52.355	6.541	47.722	5.963	43.089	5.384
0.08	54.585	6.820	50.205	6.273	45.826	5.726	41.447	5.179
0.1	51.195	6.397	47.233	5.901	43.270	5.406	39.308	4.911
0.15	41.771	5.219	39.046	4.879	36.320	4.538	33.594	4.197
0.2	34.468	4.307	32.734	4.090	31.001	3.873	29.268	3.657
0.3	27.043	3.379	26.336	3.291	25.629	3.202	24.923	3.114
0.4	24.179	3.021	23.873	2.983	23.567	2.945	23.261	2.906
0.5	22.891	2.860	22.767	2.845	22.643	2.829	22.520	2.814
0.6	22.229	2.777	22.200	2.774	22.170	2.770	22.141	2.766
0.8	21.596	2.698	21.657	2.706	21.718	2.714	21.779	2.721
1	21.310	2.663	21.412	2.675	21.514	2.688	21.616	2.701
1.5	21.185	2.647	21.312	2.663	21.439	2.679	21.566	2.695
2	21.505	2.687	21.608	2.700	21.710	2.713	21.813	2.725
3	22.548	2.817	22.567	2.820	22.585	2.822	22.604	2.824
4	23.681	2.959	23.609	2.950	23.537	2.941	23.465	2.932
5	25.720	3.214	25.491	3.185	25.262	3.156	25.033	3.128
6	27.353	3.418	27.001	3.374	26.649	3.330	26.297	3.286
8	28.649	3.579	28.198	3.523	27.747	3.467	27.297	3.411
10	30.887	3.859	30.259	3.781	29.632	3.702	29.004	3.624
15	33.087	4.134	35.074	4.382	37.062	4.631	39.050	4.879

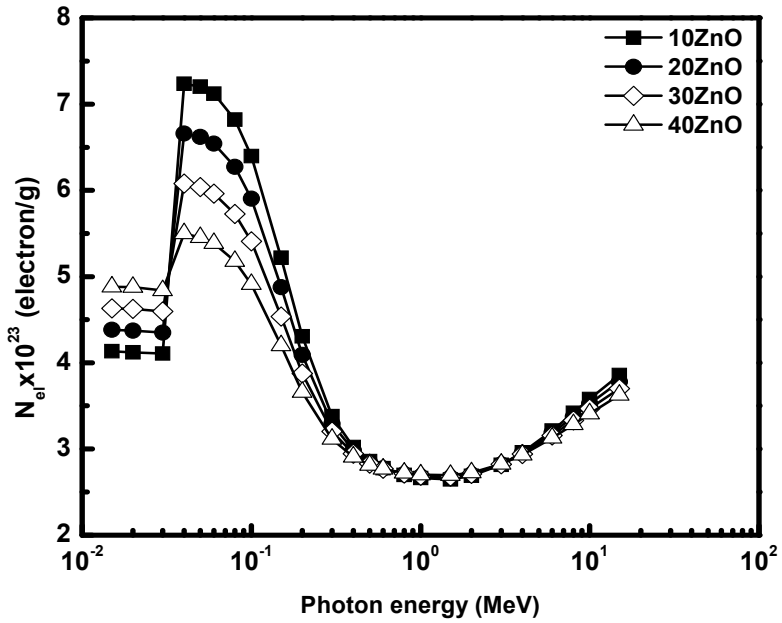

Figure 5: The variation of N_{el} with photon energy of glass samples.

4.4 Gamma Ray Buildup Factors of the Glass Samples

4.4.1 Photon energy dependence

The calculated equivalent atomic numbers (Z_{eq}) and EBF G-P fitting parameters for the glass samples in the energy range of 0.015–15 MeV are shown in Tables 5–8. Figure 6 shows the variation in the exposure buildup factor with photon energy for the glass samples at different penetration depths. It is observed that the exposure (EBF) buildup factors of the glass samples are small at both low and high energies. This may be attributed to the absorption processes, photoelectric effect and pair-production dominating at the low and high energy regions, respectively, in which photons are completely absorbed or removed. A sharp peak in the EBF values was observed at 40 keV as shown in Figure 6, which may be due to the K-absorption edge of Te at approximately 31.8 keV. Around the K-edge of high-Z elements, the mass attenuation coefficients jump to very large values at the upper side of the K-edge, and the element exhibits two mass attenuation coefficients, corresponding to the lower and upper sides of the edge. This abrupt change in the mass attenuation coefficient could lead a sharp peak in the buildup factor. The EBF values increase with increasing photon energies and show a maximum at 0.8 MeV due to multiple Compton scattering at intermediate energies. In Compton scattering, photons are not completely removed, but rather they lose energy. Finally, the EBF values begin to decrease upon further

increases in the photon energy up to 8 MeV due to pair production. We found that EBF values increased at a high energy (>8 MeV) for all of the glass samples and showed increasing penetration depths, which might be due to the increase in multiple scattering as the penetration depth increased. The EBF values were found to be in the range of 1.005–4180.6, 1.004–2730.3, 1.004–1741.2 and 1.004–1073.1 for the 10ZnO, 20ZnO, 30ZnO, and 40ZnO glass samples, respectively. The dependence on the chemical composition agreed with what was observed elsewhere.[34]

Table 5: Equivalent atomic number (Z_{eq}) and G-P exposure (EBF) buildup factor coefficients for 10ZnO-90TeO_2 glass sample.

Energy (MeV)	Z_{eq}	EBF				
		b	c	a	X_k	d
0.015	24.78	1.005	1.385	–0.449	5.861	0.312
0.02	24.89	1.013	0.182	0.547	11.307	–0.528
0.03	25.12	1.032	0.374	0.195	26.998	–0.291
0.04	44.48	3.820	0.618	0.091	24.341	–0.063
0.05	44.90	3.254	0.212	–0.088	13.814	–0.056
0.06	45.19	2.634	0.101	0.628	12.258	–0.109
0.08	45.57	1.730	0.026	0.788	14.892	–0.208
0.1	45.81	1.276	0.179	0.488	13.770	–0.238
0.15	46.16	1.229	0.401	0.231	14.165	–0.126
0.2	46.35	1.353	0.506	0.172	14.477	–0.095
0.3	46.58	1.480	0.682	0.095	14.336	–0.047
0.4	46.70	1.601	0.828	0.054	14.156	–0.039
0.5	46.78	1.672	0.912	0.033	14.163	–0.031
0.6	46.84	1.702	0.968	0.017	13.990	–0.022
0.8	46.88	1.728	1.026	0.002	14.064	–0.016
1	46.90	1.721	1.052	–0.004	13.430	–0.014
1.5	46.12	1.595	1.140	–0.025	10.981	–0.002
2	44.16	1.588	1.122	–0.020	12.758	–0.006
3	41.70	1.558	1.065	0.000	12.828	–0.028
4	40.76	1.508	1.023	0.015	13.324	–0.041
5	40.25	1.514	0.950	0.042	13.552	–0.066
6	39.90	1.487	0.931	0.052	13.738	–0.074
8	39.49	1.501	0.892	0.073	14.042	–0.091
10	39.28	1.464	0.964	0.056	14.156	–0.075
15	39.18	1.501	1.090	0.038	14.220	–0.061

Table 6: Equivalent atomic number (Z_{eq}) and G-P exposure (EBF) buildup factor coefficients for $20ZnO\text{-}80TeO_2$ glass sample.

Energy (MeV)	Z_{eq}	EBF				
		b	c	a	X_k	d
0.015	25.11	1.004	1.432	–0.477	5.791	0.323
0.02	25.22	1.012	0.166	0.569	11.332	–0.555
0.03	25.44	1.030	0.374	0.193	27.873	–0.301
0.04	42.90	3.896	0.431	0.089	23.728	–0.043
0.05	43.34	3.177	0.120	–0.209	12.835	0.003
0.06	43.66	2.528	0.055	0.851	14.732	–0.127
0.08	44.05	1.701	0.029	0.779	14.687	–0.228
0.1	44.31	1.231	0.225	0.412	13.762	–0.207
0.15	44.70	1.233	0.431	0.211	14.252	–0.113
0.2	44.91	1.392	0.509	0.172	14.417	–0.096
0.3	45.17	1.512	0.697	0.091	14.382	–0.046
0.4	45.31	1.633	0.846	0.050	14.163	–0.037
0.5	45.39	1.700	0.930	0.028	14.210	–0.029
0.6	45.44	1.728	0.984	0.013	13.976	–0.021
0.8	45.49	1.749	1.039	–0.001	14.052	–0.015
1	45.52	1.738	1.063	–0.007	13.430	–0.013
1.5	44.64	1.605	1.147	–0.027	9.640	–0.001
2	42.47	1.598	1.126	–0.021	12.651	–0.006
3	39.95	1.565	1.064	–0.001	12.755	–0.026
4	39.00	1.513	1.023	0.015	13.272	–0.039
5	38.50	1.510	0.958	0.039	13.512	–0.061
6	38.17	1.479	0.940	0.048	13.668	–0.069
8	37.77	1.480	0.901	0.068	13.964	–0.086
10	37.57	1.438	0.964	0.054	14.120	–0.072
15	37.47	1.455	1.072	0.040	14.259	–0.061

Table 7: Equivalent atomic number (Z_{eq}) and G-P exposure (EBF) buildup factor coefficients for 30ZnO-70TeO_2 glass sample.

Energy (MeV)	Z_{eq}	EBF				
		b	c	a	X_k	d
0.015	25.41	1.004	1.477	–0.504	5.725	0.333
0.02	25.53	1.012	0.152	0.590	11.355	–0.579
0.03	25.74	1.029	0.374	0.191	28.675	–0.310
0.04	41.31	3.811	0.322	0.095	22.971	–0.035
0.05	41.75	3.077	0.043	–0.308	11.975	0.053
0.06	42.08	2.414	0.007	1.091	17.382	–0.147
0.08	42.49	1.671	0.032	0.770	14.470	–0.249
0.1	42.77	1.183	0.275	0.331	13.754	–0.173
0.15	43.17	1.238	0.464	0.191	14.346	–0.100
0.2	43.38	1.434	0.511	0.173	14.352	–0.098
0.3	43.67	1.548	0.714	0.086	14.432	–0.044
0.4	43.81	1.667	0.866	0.045	14.170	–0.036
0.5	43.93	1.731	0.951	0.023	14.261	–0.027
0.6	43.97	1.756	1.000	0.009	13.961	–0.020
0.8	44.04	1.771	1.053	–0.004	14.039	–0.014
1	44.02	1.757	1.075	–0.009	13.430	–0.012
1.5	42.93	1.616	1.155	–0.029	8.171	0.000
2	40.79	1.609	1.127	–0.021	12.312	–0.005
3	38.19	1.572	1.063	–0.001	12.678	–0.025
4	37.27	1.518	1.023	0.014	13.218	–0.037
5	36.44	1.505	0.966	0.035	13.472	–0.056
6	36.44	1.471	0.949	0.043	13.595	–0.063
8	36.12	1.458	0.912	0.063	13.884	–0.081
10	35.89	1.411	0.964	0.052	14.082	–0.070
15	35.80	1.408	1.054	0.042	14.298	–0.062

Table 8: Equivalent atomic number (Z_{eq}) and G-P exposure (EBF) buildup factor coefficients for 40ZnO-60TeO_2 glass sample.

Energy (MeV)	Z_{eq}	EBF				
		b	c	a	X_k	d
0.015	25.70	1.004	1.518	–0.528	5.664	0.342
0.02	25.82	1.012	0.138	0.608	11.377	–0.602
0.03	26.03	1.020	0.374	0.190	29.160	–0.314
0.04	39.66	3.492	0.323	0.111	21.988	–0.042
0.05	40.11	2.856	0.077	–0.248	12.075	0.031
0.06	40.44	2.275	0.041	1.015	17.114	–0.147
0.08	40.85	1.626	0.064	0.724	14.368	–0.245
0.1	41.13	1.165	0.312	0.283	13.758	–0.152
0.15	41.55	1.249	0.495	0.172	14.407	–0.089
0.2	41.79	1.477	0.518	0.171	14.281	–0.098
0.3	42.08	1.587	0.732	0.080	14.487	–0.043
0.4	42.24	1.705	0.888	0.039	14.179	–0.034
0.5	42.34	1.766	0.973	0.017	14.318	–0.024
0.6	42.40	1.788	1.019	0.005	13.944	–0.019
0.8	42.47	1.796	1.068	–0.007	14.024	–0.013
1	42.49	1.777	1.088	–0.012	13.430	–0.011
1.5	41.41	1.628	1.162	–0.030	7.557	0.001
2	38.94	1.620	1.126	–0.021	11.860	–0.005
3	36.42	1.580	1.063	–0.002	12.597	–0.023
4	35.53	1.524	1.023	0.013	13.161	–0.035
5	35.08	1.500	0.974	0.031	13.429	–0.051
6	34.78	1.462	0.959	0.039	13.519	–0.058
8	34.44	1.436	0.922	0.058	13.802	–0.075
10	34.26	1.385	0.963	0.050	14.045	–0.067
15	34.17	1.360	1.035	0.044	14.338	–0.062

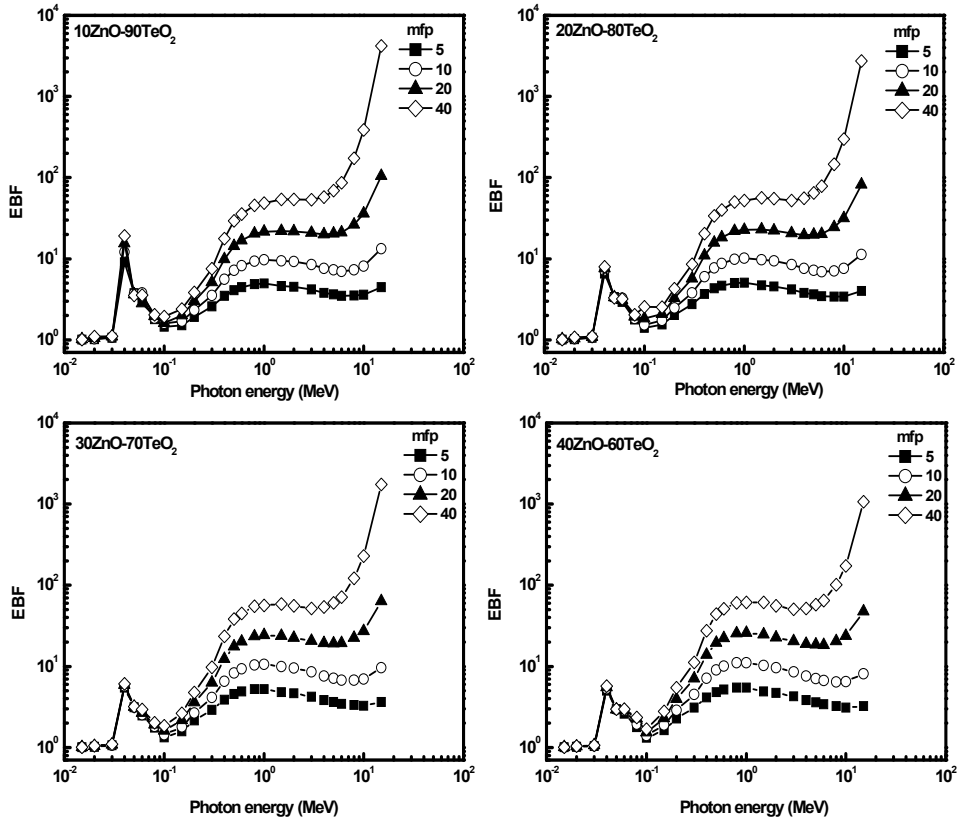

Figure 6: The exposure buildup factor (EBF) for the glass samples in the energy region 0.015–15 MeV at different penetration depth.

4.4.2 Penetration depth dependency

Figure 7 shows the variation of the EBF with penetration depth for four incident photon energies (0.015, 0.15, 1.5, and 15 MeV). It is clear that the of EBF values increased with increasing penetration depth for the glass samples. At low penetration depths, up to 3 mfp and 0.15 MeV incident photon energy, the EBF values remained constant with increasing ZnO content. At a photon energy of 1.5 MeV, the EBF values remained constant with increasing ZnO content and penetration depths up to 20 mfp. This may be due to the domination of photoelectric absorption, which depends on Z_{eq}^{4-5} at photon energies below 0.15 MeV. In the high photon energy region (>2 MeV), another absorption process, pair and triplet production, overwhelms the Compton scattering.

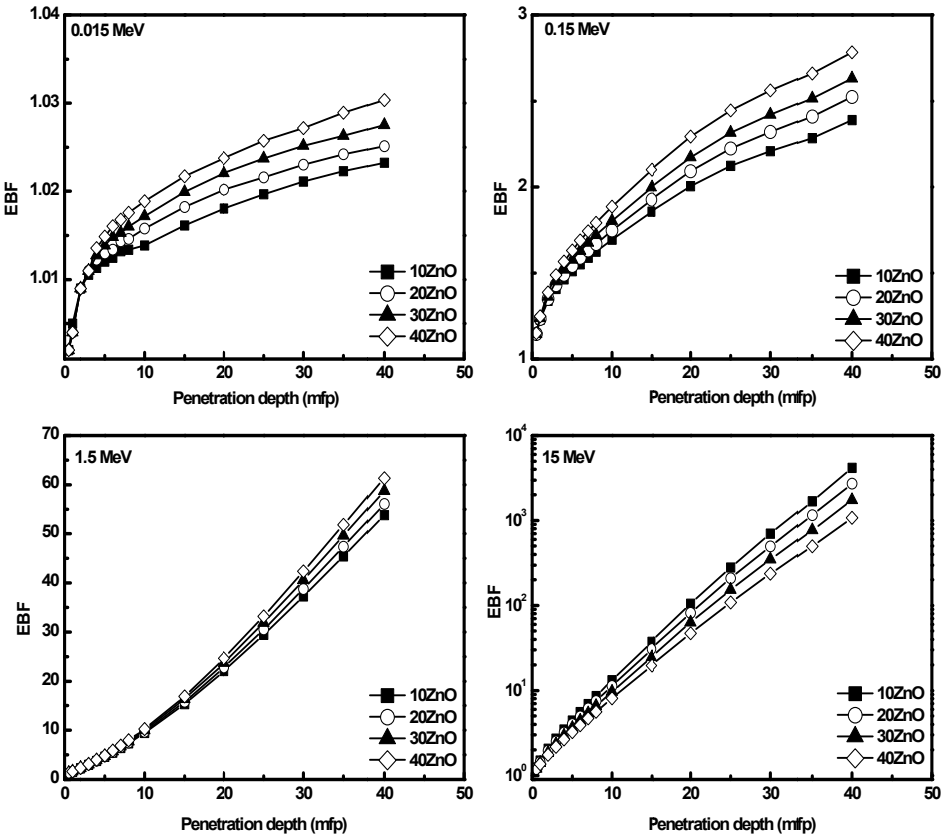

Figure 7: The exposure buildup factor for the glass samples up to 40 mfp at 0.015, 0.15, 1.5, 15 MeV.

5. CONCLUSION

The mass attenuation coefficient (μ_m), half-value layer (HVL) and mean free path for xZnO-(100-x)TeO_2 glasses, where x = 10, 20, 30 and 40 mol.%, have been measured for 0.662, 1.173 and 1.33 MeV emitted from ^{137}Cs and ^{60}Coby using a 3 × 3 inch NaI(Tl) detector. The experimental mass attenuation coefficients were found to decrease with increasing gamma ray energy and increase with increasing ZnO concentration. The half-value layer and mean free path at selected photon energies increased with increasing gamma energy and decreased with increasing ZnO concentration. The results show that the values of the mean free path of glass samples are lower than those of ilmenite, basalt-magnetite, haematite-serpentine, and ordinary concretes at photon energies of 0.662, 1.173, and 1.33 MeV. The effective atomic numbers (Z_{eff}) and electron densities (N_{el}) of the glass

samples were calculated in the photon energy range of 0.015–15 MeV and were found to be clearly energy dependent. The G-P fitting method has been used for the calculation of the exposure and buildup factors of the glass samples in the energy range 0.015–15 MeV up to 40 penetration depths. The 10ZnO-90TeO_2 glass sample was found to have lower values of the gamma ray exposure buildup factor in the intermediate energy region. The EBF was found to be energy and penetration depth dependent as well.

6. ACKNOWLEDGEMENT

This work was carried out using the analytical facilities at the Physics Department, Faculty of Sciences, Al-Azhar University, Assiut, Egypt and Physics Department, Faculty of Science, University of Tabuk, Saudi Arabia.

7. REFERENCES

1. Kaur, K., Singh, K. J. & Anand, V. (2015). Correlation of gamma ray shielding and structural properties of PbO-BaO-P_2O_5 glass system. *Nucl. Eng. Des.*, 285, 31–38, http://dx.doi.org/10.1016/j.nucengdes.2014.12.033.
2. Saeed, A. et al. (2014). Gamma ray attenuation in a developed borate glassy system. *Radiat. Phys. Chem.*, 102, 167–170, http://dx.doi.org/10.1016/j.radphyschem.2014.04.032.
3. Singh, K. J., Kaur, S. & Kaundal, R. S. (2014). Comparative study of gamma ray shielding and some properties of PbO-SiO_2-Al_2O_3 and Bi_2O_3-SiO_2-Al_2O_3 glass systems. *Radiat. Phys. Chem.*, 96, 153–157, http://dx.doi.org/10.1016/j.radphyschem.2013.09.015.
4. Singh, V. P. et al. (2014). Evaluation of gamma-ray exposure buildup factors and neutron shielding for bismuth borosilicate glasses. *Radiat. Phys. Chem.*, 98, 14–21, http://dx.doi.org/10.1016/j.radphyschem.2013.12.029.
5. Wang, J., Vogel, E. & Snitzer, E. (1994). Tellurite glass: A new candidate for fiber devices. *Opt. Mater.*, 3, 187–203, http://dx.doi.org/10.1016/0925-3467(94)90004-3.
6. Ulrich, D. R. (1964). Electrical and infrared properties of glasses in the system Bi_2O_3-TeO_2. *J. Am. Ceram. Soc.*, 47, 595–596, http://dx.doi.org/10.1111/j.1151-2916.1964.tb13828.x.
7. Burger, H. et al. (1992). Glass formation, properties and structure of glasses in the TeO_2-ZnO system. *J. Non-Cryst. Solids*, 151, 134–142.

8. Murugan, G. S. et al. (2004). Second-harmonic generation in transparent surface crystallized glasses in the $BaO-B_2-O_3-TeO_2$ system. *Appl. Phys. Lett.*, 85, 3405, http://dx.doi.org/10.1063/1.1808873.
9. Manikandan, N., Ryasnyanskiy, A. & Toulouse, J. (2012). Thermal and optical properties of TeO_2-ZnO-BaO glasses. *J. Non-Cryst. Solids*, 358, 947–951, http://dx.doi.org/10.1016%2Fj.jnoncrysol.2012.01.003.
10. Sekiya, T., Mochida, N. & Ohtsuka, A. (1994). Raman spectra of MO—TeO_2 (M = Mg, Sr, Ba and Zn) glasses. *J. Non-Cryst. Solids*, 168, 106–114, http://dx.doi.org/10.1016/0022-3093(94)90125-2.
11. Sekiya, T. et al. (1992). Raman spectra of $MO_{1/2}$-TeO_2 (M = Li, Na, K, Rb, Cs and Tl) glasses. *J. Non-Cryst. Solids*, 144, 128–144, http://dx.doi.org/10.1016/S0022-3093(05)80393-X.
12. Sharaf, J. M. & Saleh, H.(2015). Gamma-ray energy buildup factor calculations and shielding effects of some Jordanian building structures. *Radiat. Phys. Chem.*,110, 87–95, http://dx.doi.org/10.1016/j.radphyschem.2015.01.031.
13. Salehi, D., Sardari, D. & Jozani, M. (2015). Investigation of some radiation shielding parameters in soft tissue. *J. Radiat. Res. Appl. Sci.*, 8, 439–445, http://dx.doi.org/10.1016/j.jrras.2015.03.004.
14. Harima, Y. et al. (1986). Validity of the geometric-progression formula in approximating gamma-ray buildup factors. *Nucl. Sci. Eng.*, 94, 24–35.
15. Suteau, C. (2005). An iterative method for calculating gamma-ray build-up factors in multi-layer shields. *Radiat. Prot. Dosim.*, 116, 489–492, http://dx.doi.org/10.1093/rpd/nci192.
16. Shimizu, A. (2002). Calculation of gamma-ray buildup factors up to depths of 100 mfp by the method of invariant embedding. (I). Analysis of accuracy and comparison with other data. *J. Nucl. Sci. Technol.*, 39, 477–486, http://dx.doi.org/10.1080/18811248.2002.9715225.
17. Shimizu, A., Onda, T. & Sakamoto, Y. (2004). Calculation of gamma-ray buildup factors up to depths of 100 mfp by the method of invariant embedding. (III). Generation of an improved data set. *J. Nucl. Sci. Technol.*, 41, 413–424, http://dx.doi.org/10.1080/18811248.2004.9715503.
18. Sardari, D. et al. (2009). Estimation of gamma- and X-ray photons buildup factor in soft tissue with Monte Carlo method. *Appl. Radiat. Isot.*, 67, 1438–1440, http://dx.doi.org/10.1016/j.apradiso.2009.02.033.
19. American National Standard, ANS. (1991). *ANSI/ANS-6.4.3: Gamma ray attenuation coefficient and buildup factors for engineering materials*. New York: ANS.
20. Singh, V. P., Badiger, N. M. & Kaewkhao, J. (2014). Radiation shielding competence of silicate and borate heavy metal oxide glasses: Comparative study. *J. Non-Cryst. Solids*, 404, 167–173, http://dx.doi.org/10.1016/j.jnoncrysol.2014.08.003.

21. Chanthima, N. & Kaewkhao, J. (2013). Investigation on radiation shielding parameters of bismuth borosilicate glass from 1keV to 100GeV. *Ann.Nucl. Eng.*, 55, 23–28, http://dx.doi.org/10.1016/j.anucene.2012.12.011.
22. Singh, K. J., Kaur, S. & Kaundal, R. S. (2014). Comparative study of gamma ray shielding and some properties of PbO-SiO_2-Al_2O_3 and Bi_2O_3-SiO_2-Al_2O_3 glass systems. *Radiat. Phys. Chem.*, 96, 153–157, http://dx.doi.org/10.1016/j.radphyschem.2013.09.015.
23. Ruengsri, S. et al. (2015). Development of barium borosilicate glasses for radiation shielding materials using rice husk ash as a silica source. *Prog. Nucl. Energy*, 83, 99–104, http://dx.doi.org/10.1016/j.pnucene.2015.03.006.
24. Singh, V. P. et al. (2014). Evaluation of gamma-ray exposure buildup factors and neutron shielding for bismuth borosilicate glasses. *Radiat. Phys. Chem.*, 98, 14–21, http://dx.doi.org/10.1016/j.radphyschem.2013.12.029.
25. Kurudirek, M. (2014). Radiation shielding and effective atomic number studies in different types of shielding concretes, lead base and non-lead base glass systems for total electron interaction: A comparative study. *Nucl. Eng. Des.*, 280, 440–448, http://dx.doi.org/10.1016/j.nucengdes.2014.09.020.
26. Burger, H., Vogel, W. & Kozhukharov, V. (1985). IR transmission and properties of glasses in the TeO_2-RnOm, RnXm, Rn(SO_4)m, Rn(PO_3)m and [B_2O_3] systems. *Infrared Phys.*, 25, 395–409, http://dx.doi.org/10.1016/0020-0891(85)90114-9.
27. Sidek, H. et al. (2004). Formation and elastic behavior of lead-magnesium chlorophosphate glasses. *Turkish J. Phys.*, 28, 65–71.
28. Sidek, H. et al. (2009). Synthesis and optical properties of ZnO-TeO_2 glass system. *Am. J. App. Sci.*, 6, 1489–1494, http://dx.doi.org/10.3844/ajassp.2009.1489.1494.
29. Gerward, L. et al. (2001). X-ray absorption in matter. Reengineering XCOM. *Radiat. Phys. Chem.*, 60, 23–24, http://dx.doi.org/10.1016/S0969-806X(00)00324-8.
30. Gerward, L. et al. (2004). WinXCom - A program for calculating X-ray attenuation coefficients. *Radiat. Phys. Chem.*, 71, 653–654, http://dx.doi.org/10.1016/j.radphyschem.2004.04.040.
31. Harima, Y. (1983). An approximation of gamma-ray buildup factors by modified geometrical progression. *Nucl. Sci. Eng.*, 83, 299–309.
32. Harima, Y. (1993). An historical review and current status of buildup factor calculations and applications. *Radiat. Phys. Chem.*, 41, 631–672, http://dx.doi.org/10.1016/0969-806X(93)90317-N.

33. Bootjomchai, C. et al. (2012). Gamma-ray shielding and structural properties of barium-bismuth-borosilicate glasses. *Radiat. Phys. Chem.*, 81, 785–790, http://dx.doi.org/10.1016/j.radphyschem.2012.01.049.
34. Kurudirek, M. & Zdemir, Y. (2011). Energy absorption and exposure buildup factors for some polymers and tissue substitute materials: Photon energy, penetration depth and chemical composition dependence. *J. Radiol. Prot.*, 31, 117–128, http://dx.doi.org/10.1088/0952-4746/31/1/008.